

Improved spectral analysis for the motional Stark effect diagnostic

J. Ko and J. Klabacha

Citation: *Rev. Sci. Instrum.* **83**, 10D513 (2012); doi: 10.1063/1.4733546

View online: <http://dx.doi.org/10.1063/1.4733546>

View Table of Contents: <http://rsi.aip.org/resource/1/RSINAK/v83/i10>

Published by the [American Institute of Physics](#).

Related Articles

Investigating the performance of an ion luminescence probe as a multichannel fast-ion energy spectrometer using pulse height analysis

Rev. Sci. Instrum. **83**, 10D306 (2012)

Development of a mirror-based endoscope for divertor spectroscopy on JET with the new ITER-like wall (invited)

Rev. Sci. Instrum. **83**, 10D511 (2012)

Far-infrared polarimetry diagnostic for measurement of internal magnetic field dynamics and fluctuations in the C-MOD Tokamak (invited)

Rev. Sci. Instrum. **83**, 10E316 (2012)

Barrier discharges driven by sub-microsecond pulses at atmospheric pressure: Breakdown manipulation by pulse width

Phys. Plasmas **19**, 070701 (2012)

Solid debris collection for radiochemical diagnostics at the National Ignition Facility

Rev. Sci. Instrum. **83**, 10D904 (2012)

Additional information on *Rev. Sci. Instrum.*

Journal Homepage: <http://rsi.aip.org>

Journal Information: http://rsi.aip.org/about/about_the_journal

Top downloads: http://rsi.aip.org/features/most_downloaded

Information for Authors: <http://rsi.aip.org/authors>

ADVERTISEMENT



Special Topic Section:
PHYSICS OF CANCER

Why cancer? Why physics? [View Articles Now](#)

Improved spectral analysis for the motional Stark effect diagnostic^{a)}

J. Ko^{1,2,b)} and J. Klabacha¹

¹*Department of Physics, University of Wisconsin-Madison, Madison, Wisconsin 53706, USA*

²*National Fusion Research Institute, Daejeon 305-806, Korea*

(Presented 8 May 2012; received 8 May 2012; accepted 14 June 2012;
published online 13 July 2012)

The magnetic pitch angle and the magnitude from reversed field pinch plasmas in the Madison symmetric torus (MST) have been routinely obtained from fully resolved motional Stark effect (MSE) spectrum analyses. Recently, the spectrum fit procedure has been improved by initializing and constraining the fit parameters based on the MSE model in the atomic data and analysis structure. A collisional-radiative model with level populations n -resolved up to $n = 4$ and a simple Born approximation for ion-impact cross sections is used for this analysis. Measurement uncertainty is quantified by making MSE measurements with multiple views of a single spatial location, ranging 5%–15% for typical MST operation conditions. A multi-view fit improves the goodness of fit of MSE spectral features and background. © 2012 American Institute of Physics. [<http://dx.doi.org/10.1063/1.4733546>]

I. INTRODUCTION

A precise and reliable spectral motional Stark effect (MSE) diagnostic could complement and calibrate the conventional polarimetric approach¹ in an environment where direct polarization measurements are difficult or may be compromised (e.g., the device for the International Thermonuclear Experimental Research (ITER)).^{2,3} Low-magnetic-field (0.2–0.6 T) MSE spectra are routinely obtained with high-time resolution from reversed field pinch (RFP) plasmas in the Madison symmetric torus (MST),⁴ which makes MST a good test bed for investigating the fully spectral MSE approach and the relevant atomic physics. Because the MSE diagnostic at MST deals with Stark spectra generated under such low magnetic fields, in principle the analysis should rely on an atomic model that includes spin-orbit coupling, Zeeman effects, and non-statistical populations of upper states in diagnostic-neutral-beam excitation. However, no current atomic model has been validated as reliable for these low-field MSE spectra. A recent collisional radiative model^{5,6} confirms that observed Stark multiplets deviate from a statistical population but calculations were done only at high fields (>1 T).

Recent improvements in the MST MSE spectrum analysis include the initialization and constraints of the fit parameters using the atomic data and analysis structure (ADAS) calculations.⁷ The relative intensities among the Stark multiplets calculated by the ADAS should not necessarily be regarded as accurate. This is due to the limitations of the MSE model used in the version of the ADAS utilized in this analysis and the uncertainties of the plasma parameters inputs (elaborated upon in Sec. II). Therefore, these intensities are only used as initial values, and are allowed to change during the fit iterations. Also the fit is done for the multiple sets of Stark multiplets collected from different fiber bundles (usually 4–6 fiber bundles) within a single CCD frame, the

schematic of which will be shown in Sec. II. The results of the new spectrum fit will be given in Sec. III and the conclusions in Sec. IV.

II. MULTIPLE SETS OF STARK MULTIPLETS IN A SPECTRUM

The original design of the MST MSE system was intended to have multiple time points by having multiple lines of sight (or views) for a single spatial location.^{8,9} This is illustrated in Figure 1 where the resultant spectra from the views are also included. There are seven views for the on-axis measurements with slightly different viewing angles among views ($\Delta\theta_{\max} \sim 6^\circ$). The shutters for these views can open at different times during one CCD frame exposure. The same is true for the off-axis (half-minor radius) measurements, except the number of views is 3–4 in this case. The gratings in the spectrometer are adjusted such that the signals from

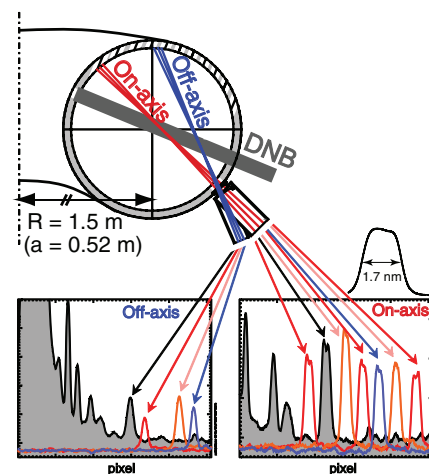


FIG. 1. MST MSE lines of sight (or views) for the on-axis and off-axis measurement locations and their typical spectra showing multiple sets of Stark multiplets. The shadowed region indicates the contributions from the reference (unfiltered) view. The filter function of the bandpass filters is also illustrated above the on-axis spectrum plot.

^{a)}Contributed paper, published as part of the Proceedings of the 19th Topical Conference on High-Temperature Plasma Diagnostics, Monterey, California, May 2012.

^{b)}Author to whom correspondence should be addressed: jinseok@nfri.re.kr.

individual views fall on to different regions of the CCD pixel array. All of the views have narrow [full width at half maximum (FWHM) ~ 1.7 nm] bandpass filters to exclude their second and third energy components (typical filter function illustrated in Figure 1). They also have some impurity line peaks (usually Carbon II), except for one view for each spatial location. This view is acting as a reference view. The signals from the reference views include peaks from all possible emissions such as thermal $D\alpha$, impurity lines, and Doppler-shifted Stark multiplets from different energy components. All of these factors are indicated as the shadowed regions in Figure 1. The reference views are used to obtain the dispersion of the spectrometer. However, the signals from the reference view significantly complicate the overall spectrum, as can also be seen in Figure 1. This is particularly important because many of the small impurity peaks from the reference views are “under” the signal peaks from the other views. This also indicates the reference view can be turned off to make the spectrum much cleaner. A separate wavelength calibration was performed using Samarium and Neon lamps, where the conversions from pixels for each view were obtained for both the dispersion and the absolute wavelength.

The ADAS MSE module used in this work (version 3.1) utilized a simple Born approximation for cross-sections for ion-impact interactions, which are the dominant interactions for the Balmer α emissions from the beam neutrals. Although the emission calculations in this module include fine structures and Zeeman effects, the levels are nlm-resolved only up to $n = 4$. Therefore, it is believed that there are systematic uncertainties in the Stark intensity calculations. Moreover, this module has not been validated with low-field (a few tenths of a Tesla) MSE spectra. The module requires some plasma and beam parameters as inputs, such as plasma density and temperature, effective ion charge (Z_{eff}), beam energy and density, etc. Not all the measurements are available at MST and many of these measurements are either line-integrated or global, whereas the ADAS calculations require local values. Therefore, it is reasonable to use the ADAS calculations as initial values for the fitting procedure but not as final values. During the initialization calculations with the ADAS, the transitions (typically 50–70 transitions at around 0.5 T) are grouped into nine lines, centered at nine main Stark transition wavelengths. These wavelengths are initially determined by speculated magnetic field strength and Doppler shift values.

Figure 2 illustrates the flow of the fitting procedure. The fitting procedure initializes the free parameters before starting the minimization. The initialization of the intensities should be performed for individual peaks because the ADAS module produces the relative Stark intensities on the real wavelength grid. After being converted into intensities on the pixel grid, they can be used in the fitting of the entire spectrum. The line broadening is initialized from the beam-into-gas shot without magnetic fields. Once the initial values are collected from all peaks, the fit starts the least square minimization procedure to find both the correct pitch angle and the Stark splitting (i.e., the magnitude of the field) as described in Ref. 10. The number of fit parameters is rather large. For each set of Stark multiplets, there are nine parameters for intensities and three common parameters for broadening, Stark splitting, and Doppler

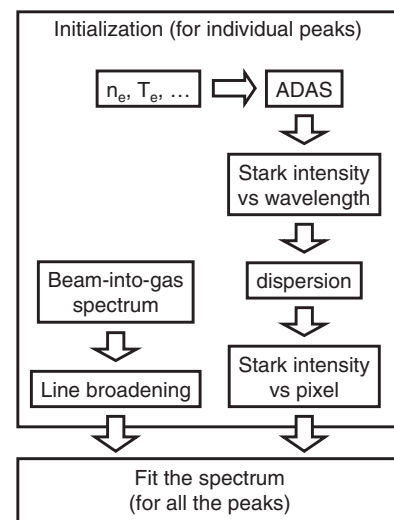


FIG. 2. The flow chart of the initialization of the Stark intensity and line broadening for the MSE spectrum fit.

shift (σ_0 location). Further, there are four more parameters from the global background polynomial and one additional parameter for the scaling factor. This results in a total of 77 free parameters in the case of using all six views (minus the reference view) from the on-axis location. Careful constraints should be made for some parameters to avoid non-physical fitting results. Each parameter has different constraints, dependent upon the amount of the parameter’s typical fluctuation when unconstrained. The results of many trials and errors suggest about 30% constraints for the Stark intensities is reasonable. Too small initial constraint (less than 10%) results in the saturation of parameters to that constraint.

III. FIT RESULTS

Figure 3 illustrates on-axis MSE spectra from three different RFP discharges with plasma currents of about 200, 350,

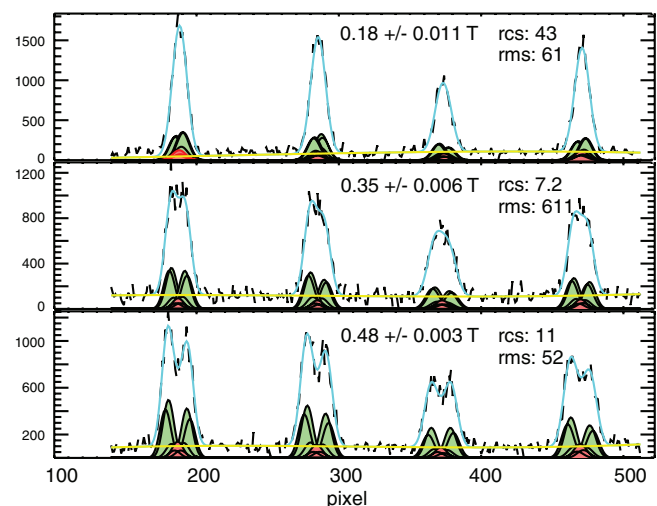


FIG. 3. MSE spectra and their fitting results for three different RFP discharges with plasma currents of 200, 350, and 500 kA (from the top to the bottom). The sigma and pi components are color coded for each Stark multiplets. The third-order polynomial background and the total spectrum fit are also shown. “rcs” and “rms” stand for reduced chi square and root-mean-square error, respectively.

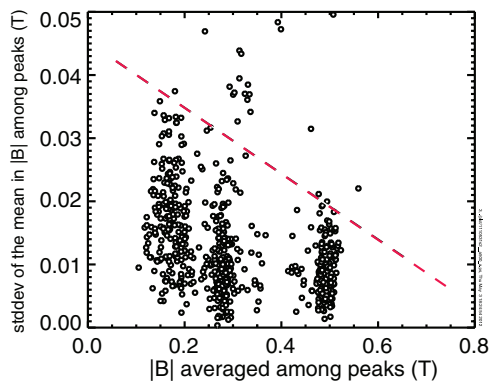


FIG. 4. Collection of measurement error as a function of $|B|$ for various RFP plasma currents (200–600 kA). The dashed line is an approximation that illustrates the rough upper bound of the uncertainties.

and 500 kA. For the plasma and beam parameters inputs to the ADAS initialization, either measurements or assumptions are used. Plasma density was line-integrated from interferometer measurements ($\sim 10^{19} \text{ m}^{-3}$) because no density profile measurements were made for these discharges. Typical MST values were used for the temperature and Z_{eff} inputs because the measurements were not available for these discharges (500 eV and 2, respectively). The sensitivities of the magnetic field obtained from the fit on temperature and Z_{eff} are rather small (less than a percent per 100% change in these parameters). However, the sensitivity of the plasma density is relatively large. It is noteworthy that the deviation becomes 2%–3% when the density input is reduced by a factor of 10 from the line-averaged density, implying the deviation from the statistical upper state population at low densities.

The results from Figure 3 show that fitting the whole spectrum can handle the background between two adjacent peaks with reasonable goodness of the fit (reduced chi square; “rcs” on the plot) and root-mean-square fit error (“rms” on the plot). The fit also describes the change in the Stark splitting along with the plasma current. In these spectra, the reference view and two more views were suppressed to minimize the peak-to-peak overlap and interference. Also, these spectra were taken at the same time by opening the shutters for these views simultaneously. This provides not only real-time peak-to-peak calibration, but also the variations among peaks can be regarded as measurement uncertainties. The average of the variations and their standard deviation of the mean are also given in Figure 3.

Figure 4 shows the measurement uncertainties inferred as a function of the magnetic fields collected from about 700 MSE frames with various plasma currents (200–600 kA;

close to the MST operation range). With higher currents (or higher magnetic fields), the peak-to-peak variation is smaller. This implies that the ADAS model becomes less reliable with lower magnetic fields. The result sets the upper bounds of the measurement uncertainties (marked as the dashed line on the plot) as 5%–15% for 0.6–0.2 T. Following the sensitivity study for the MSE constraints on the RFP magnetic equilibria,¹⁰ this upper bound propagates to be less than 10% in the central parallel current density and less than 5% in the central safety factor.

IV. CONCLUSIONS

The MSE fitting scheme has been improved for the MST RFP plasmas. The initialization of the free parameters with the values which are close to their real physical values, assisted by the MSE model in the ADAS has made it possible to solve the complicated many-free-parameter (~ 80) fitting problems. The unique feature of the MSE data acquisition associated with the whole-spectrum fitting scheme enables one to estimate experimental uncertainties that seem to be acceptable for the MST RFP equilibrium reconstruction.

ACKNOWLEDGMENTS

Authors thank to Dr. Daniel Den Hartog for his guidance and advice in this work. This work was supported by the U.S. Department of Energy (DOE) under Contract No. DE-FC02-05ER54814.

¹F. M. Levinton, *Phys. Rev. Lett.* **63**, 2060 (1989).

²M. Kuldkepp, E. Rachlew, N. C. Hawkes, and B. Schunke, *Rev. Sci. Instrum.* **75**, 3446 (2004).

³E. L. Foley, F. M. Levinton, H. Y. Yuh, and L. E. Zakharov, *Rev. Sci. Instrum.* **79**, 10F521 (2008).

⁴D. J. Den Hartog, J. R. Ambuel, M. T. Borchardt, K. J. Caspary, E. A. Den Hartog, A. F. Falkowski, W. S. Harris, J. Ko, N. A. Pablant, J. A. Reusch, P. E. Robl, H. D. Stephens, H. P. Summers, and Y. M. Yang, *Fusion Sci. Technol.* **59**, 124 (2011).

⁵O. Marchuk, Yu Ralchenko, R. K. Janev, W. Biel, E. Delabie, and A. M. Urmov, *J. Phys. B* **43**, 011002 (2010).

⁶E. Delabie, M. Brix, C. Giroud, R. J. E. Jaspers, O. Marchuk, M. G. O’Mullane, Yu Ralchenko, E. Surrey, M. G. von Hellermann, K. D. Zastrow, and JET-EFDA Contributors, *Plasma Phys. Controlled Fusion* **52**, 125008 (2010).

⁷H. P. Summers, *The ADAS Manual*, version 2.6, 2004, see <http://www.adas.ac.uk>.

⁸D. Craig, D. J. Den Hartog, and G. Fiksel, *Rev. Sci. Instrum.* **72**, 1008 (2001).

⁹D. J. Den Hartog, D. Craig, D. A. Ennis, G. Fiksel, S. Gangadhara, D. J. Holly, J. C. Reardon, V. I. Davydenko, A. A. Ivanov, A. A. Lizunov, M. G. O’Mullane, and H. P. Summers, *Rev. Sci. Instrum.* **77**, 10F122 (2006).

¹⁰J. Ko, D. J. Den Hartog, K. J. Caspary, E. A. Den Hartog, N. A. Pablant, and H. P. Summers, *Rev. Sci. Instrum.* **81**, 10D702 (2010).